frontiers | Frontiers in Pharmacology

TYPE Original Research
PUBLISHED 31 October 2022
DOI 10.3389/fphar.2022.899628

OPEN ACCESS

EDITED BY
Nelson Chong,
Nottingham Trent University,
United Kingdom

REVIEWED BY
Yasufumi Shigeyoshi,
Kindai University, Japan
Masashi Mukohda,
Okayama University of Science, Japan

*CORRESPONDENCE
Lilei Zhang,
lilei.zhang@bcm.edu
Zheng Sun,
zheng.sun@bcm.edu

†These authors have contributed equally to this work

SPECIALTY SECTION
This article was submitted to Cardiovascular and Smooth Muscle Pharmacology, a section of the journal Frontiers in Pharmacology

RECEIVED 18 March 2022
ACCEPTED 10 October 2022
PUBLISHED 31 October 2022

CITATION
Luo X, Song S, Qi L, Tien C-L, Li H, Xu W, Mathuram TL, Burris T, Zhao Y, Sun Z and Zhang L (2022), REV-ERB is essential in cardiac fibroblasts homeostasis. *Front. Pharmacol.* 13:899628. doi: 10.3389/fphar.2022.899628

REV-ERB is essential in cardiac fibroblasts homeostasis

Xiaokang Luo[1†], Shiyang Song[2†], Lei Qi[1†], Chih-Liang Tien[1], Hui Li[1], Weiyi Xu[1], Theodore Lemuel Mathuram[1], Thomas Burris[3], Yuanbiao Zhao[1], Zheng Sun[2,4]* and Lilei Zhang[1]*

[1]Department of Molecular and Human Genetics, Baylor College of Medicine, Houston, TX, United States, [2]Department of Medicine, Division of Diabetes, Endocrinology and Metabolism, Baylor College of Medicine, Houston, TX, United States, [3]Genetics Institute, University of Florida, Gainesville, FL, United States, [4]Department of Molecular and Cellular Biology, Baylor College of Medicine, Houston, TX, United States

REV-ERB agonists have shown antifibrotic effects in the heart and other organs. The function of REV-ERB in the cardiac fibroblasts remains unstudied. Here, we characterize the functional difference of REV-ERB in mouse embryonic fibroblasts and cardiac fibroblasts using genetic deletion of REV-ERBα and *ß in vitro*. We show that REV-ERB α/β double deleted cardiac fibroblasts have reduced viability and proliferation, but increased migration and myofibroblasts activation. Thus, REV-ERB α/β has essential cell-autonomous role in cardiac fibroblasts in maintaining them in a healthy, quiescent state. We also show that existing REV-ERB agonist SR9009 strongly suppresses cardiac fibroblasts activation but in a REV-ERB-independent manner highlighting the need to develop novel REV-ERB agonists for treating cardiac fibrosis.

KEYWORDS

REV-ERB, fibroblast activation, SR9009, cardiac fibroblasts, TGFβ

Introduction

The mammalian behavioral and physiological processes follow a 24-h cycle. While the central clock exists in the suprachiasmatic nucleus (SCN) of the brain, the molecular circadian clock is ubiquitously expressed in almost all cell types throughout the body and can operate as peripheral clocks independently of the SCN central clock. Cell type-specific deletion of the clock genes in peripheral tissues has provided critical insights into the function of the peripheral clocks. Cardiomyocyte-specific deletion of the core clock gene BMAL1 show age-associated dilated cardiomyopathy (Lefta et al., 2012; Young et al., 2014; Ingle et al., 2015). Nuclear receptor REV-ERBα and *ß* are encoded by *Nr1d1* and *Nr1d2* genes, respectively. REV-ERBs act as transcription suppressors of the second feedback loop in the core clock (Takahashi, 2017). We and others have recently reported that double deletion of REV-ERBα/β in the cardiomyocytes leads to progressive dilated cardiomyopathy and lethal heart failure, suggesting a critical function of REV-ERB in the cardiomyocytes (Dierickx et al., 2022; Song et al., 2022).

Cardiomyocytes constitute ~30–40% of the cells in the heart (Pinto et al., 2016; Zhou and Pu, 2016). Many other cell types in the heart have critical functions in cardiac

physiology and disease pathogenesis. Cardiac fibroblasts (CFs) activation by various signaling pathways, including the TGF-β pathway, results in cardiac fibrosis and is a well-recognized etiological factor in ischemic heart disease, hypertensive heart disease, hypertrophic cardiomyopathy, and dilated cardiomyopathy (Frohlich, 2001; Jellis et al., 2010; Travers et al., 2016; Disertori et al., 2017). The role of REV-ERB in CFs has not been investigated.

SR9009 is a REV-ERB agonist with various health benefits in different experimental systems (Banerjee et al., 2014; Zhang et al., 2017; Gonzalez-Fernandez et al., 2018; Griffett et al., 2020; Wolff et al., 2020). SR9009 is cardioprotective in myocardial infarction (MI) mice models (Stujanna et al., 2017; Reitz et al., 2019). We have shown that SR9009 can protect the heart in a pressure-overload model by preserving cardiac function, reducing cardiac fibrosis, and limiting pathological remodeling (Zhang et al., 2017). It is unknown whether the reduced cardiac fibrosis is due to reduced cardiac injury *via* a cross-talk between cardiomyocytes and CFs (Manabe et al., 2002; Kakkar and Lee, 2010) or whether SR9009 has a direct effect on CFs.

REV-ERB likely plays a role in the fibroblasts because SR9009 reduces acute cigarette smoke-induced inflammatory response and abnormal epithelial-to-mesenchymal transition in the lung (Wang et al., 2021). SR9009 also suppresses hepatic fibrosis in a non-alcoholic steatotic hepatitis murine model (Griffett et al., 2020). Another REV-ERB agonist GSK4112 inhibits myofibroblasts activation in idiopathic pulmonary fibrosis (IPF) fibroblasts (Cunningham et al., 2020). However, SR9009 has REV-ERB–independent effects in the mouse hepatocytes, embryonic stem cells and cardiomyocytes (Li et al., 2022) (Dierickx et al., 2019). Therefore, it is unclear whether REV-ERB has a cell-autonomous function in fibroblasts and whether the effect of SR9009 in fibroblasts is dependent on REV-ERB. Here, we use genetic approaches to investigate the function of REV-ERB in two different fibroblastic cell types, mouse embryonic fibroblasts (MEFs) and CFs. We also addressed the REV-ERB dependency of SR9009 in those fibroblasts.

Materials and methods

Mice

REV-ERBα and *ß* floxed mice were previously described (Rev-erbα^{loxP} (*Nr1d1*$^{tm1.2Rev}$, MGI ID 5426700) and Rev-erbβ^{loxP} (*Nr1d2*$^{tm1.1Rev}$, MGI ID 5426699) (Song et al., 2022). They were crossed to generate the double floxed mouse line (*Nr1d1/2*$^{fl/fl}$). The exon three and exon four of *Nr1d1* were floxed, which will lead to an in-frame deletion of the DNA binding domain upon Cre recombinase cleavage (Cho et al., 2012). The exon three of *Nr1d2* was floxed, which leads to a frame-shift deletion and nonsense-mediated decay of the transcript upon Cre recombinase cleavage (Cho et al., 2012). All the animal procedures were approved by the Institutional Animal Care and Use Committee at Baylor College of Medicine.

Fibroblasts cultures and treatments

MEFs were isolated at E13.5 as previously described (Durkin et al., 2013). CFs were isolated from 8 to 12 weeks old adult mice or from Sprague-Dawley rat pups at postnatal day 2 as previously described (Karch et al., 2019). MEFs at passages five to six or CFs at passages one to two were used for the experiments. To induce REV-ERB deletion, Cre Recombinase expressing adenovirus (Ad-Cre-GFP, with GFP reporter, Vector Biolabs, PA, United States) was transduced to cultured fibroblasts (MEFs and CFs) at a Multiplicity of Infection (MOI) rate of 400. The vector expressing GFP alone (Ad-GFP, Vector Biolabs, PA, United States) was used as the control. *Fibroblasts (MEFs and CFs) were cultured in DMEM* (*high glucose,* Thermo Fisher, with 10% fetal bovine serum, FBS), then switched to *low* serum condition (FBS, 0.1%) for 24 h prior to *activation*. *TGF-β1* (*10 mg/ml, R&D Systems, MN, United States*) *was added to the low-serum DMEM for 48hrs to induce the activation of fibroblasts to myofibroblasts.* The REV-ERB agonist SR9009 was given at a concentration of 10 μM when indicated.

Immunofluorescence staining

Coverslips with fibroblasts culture were fixed with 100% methanol for 15 min. The cells were incubated with primary antibody against α-smooth muscle actin (ab5694, Abcam, 1: 100 dilution) at 4°C overnight after blocking. Then, the cells were incubated with a fluorescence conjugated secondary antibody (A-11037, Invitrogen, 1:500 dilution) for 1 h in the dark and stained with DAPI (D3571, Invitrogen). Images were captured with EVOS FL Auto Imaging System (Life Technologies, Thermo Fisher Scientific, Inc.) and analyzed using ImageJ (National Institute of Health, United States).

Reverse transcription and quantitative real-time PCR

Total RNA was extracted using a High Pure RNA Isolation Kit (Roche, Mannheim, Germany) according to the manufacturer's protocol. The concentration was measured by a microplate reader (FLUOstar Omega, BMG LABTECH, Ortenberg, Germany). cDNA was synthesized using a reverse transcription supermix (iScript, BIO-RAD, CA, United States). Quantitative real-time PCR was performed on QuantStudio five Dx Real-Time PCR Systems (Applied Biosystems, Thermo Fisher Scientific, Inc.) with SYBR Green Supermix (SSO Advanced, BIO-RAD, CA, United States). All

TABLE 1 Primers used for qRT-PCR.

Gene	Sequence
Nr1d1 exon 4-F	CATGCCAACGGAGAGACACT
Nr1d1 exon 4-R	GCCGGAGCATCCAACAGAAT
Nr1d1-F	ACGACCCTGGACTCCAATAA
Nr1d1-R	CCATTGGAGCTGTCACTGTAGA
Nr1d2 exon 3-F	AGTGGCATGGTTCTACTGTGT
Nr1d2 exon 3-R	GCCTTCACAAGCATGAACTCC
Nr1d2-F	CAGACTGAGAACAGAAATAGTTACCTG
Nr1d2-R	GAGACTTGCTCATAGGACACACC
Acta2-F	ACTGGGACGACATGGAAAAG
Acta2-R	GTTCAGTGGTGCCTCTGTCA
Col1a1-F	GCTCCTCTTAGGGGCCACT
Col1a1-R	CCACGTCTCACCATTGGGG
Fn1-F	ATGTGGACCCCTCCTGATAGT
Fn1-R	GCCCAGTGATTTCAGCAAAGG
Ppib-F	TTCTTCATAACCACAGTCAAGACC
Ppib-R	ACCTTCCGTACCACATCCAT

primers used in this manuscript are listed in Table 1. *Ppib* was used as a reference for normalization. The relative mRNA expression was calculated by the ΔΔCt method.

BrdU incorporation assay

The fibroblast DNA synthesis and proliferation was evaluated by BrdU Cell Proliferation Assay Kit (Cell Signaling Technology. Inc., MA, United States) following the manufacturer's manual. Cells were incubated with BrdU for 6 h prior to the assay. The absorbance was measured at 450 nm by a microplate reader (FLUOstar Omega, BMG LABTECH, Ortenberg, Germany).

Cell proliferation and cytotoxicity assay

The proliferation ability of CFs was assessed by Cell Counting Kit 8 (CCK-8, 96992-100TESTS-F Sigma) following the manufacturer's manual. Cells were incubated with WST-8 (tetrazolium salt, Patent No. WO97/38985) Solution for 5 h prior to the assay.

Wound healing assay

In order to study the dynamics of fibroblast activation during wound closure, CFs were seeded in monolayers and tested by the scratch assay as previously described (Liang et al., 2007). Images were acquired before and after scratch at multiple time points up to 36 h and analyzed by measuring the average distance of the gap by ImageJ (National Institute of Health, United States). For a single time point study, the residue wound is measured at a predetermined time point (18 h) and compared. For a multiple time point healing kinetics study, the cells were examined 5 times after the scratch wound for 24–36 h till complete closure of the wound.

Immunoblotting

Cells were lysed in RIPA buffer supplemented with a complete protease inhibitor cocktail (Roche) and PhosSTOP (Roche). Lysates were resolved by gel electrophoresis (Bio-Rad), transferred to PVDF membranes (Immubilon-P, Millipore), and probed with the following antibodies: anti-REV-ERBα (1:500 (E1Y6D) Cell signaling, #13418), and anti-GAPDH (1:1,000, Cell signaling, #97166).

Statistical analysis

Data was shown as means ± *SEM*. Comparisons were analyzed by Student's t test, one-way ANOVA, or two-way analysis of variance (ANOVA). Multiple comparisons were taken into account when necessary. All statistical analysis was performed on IBM SPSS Statistics 22.0 (Armonk, NY, United States) or GraphPad Prism (San Diego, CA, United States). $p < 0.05$ was considered statistically significant. Experiments were repeated at least three times independently.

Results

Generation of the *Nr1d1/Nr1d2* double deletion MEFs model

To study the REV-ERB function in the fibroblast, we isolated MEFs from the previously reported *Nr1d1*$^{tm1.2Rev}$ and *Nr1d2*$^{tm1.1Rev}$ double floxed mouse line (Song et al., 2022). We infected the MEFs with either Cre expressing (Ad-Cre-GFP) or control (Ad-GFP) adenovirus (Figure 1A). Percent GFP positive cells showed a near 100% infection efficiency. Cre induced deletion was validated by qRT-PCR, and the results showed an 89% reduction of *Nr1d1* and an 82% reduction of *Nr1d2* in the Ad-Cre-GFP infected MEFs (which we denoted as double knockout or DKO for simplicity) compared to the ad-GFP infected MEFs (double floxed controls, *Nr1d1/2*$^{fl/fl}$) (Figures 1B–D).

Double deletion of *Nr1d1/Nr1d2* has no effect on MEFs activation

To examine the effect of REV-ERB on MEFs activation, we treated *Nr1d1/2*$^{fl/fl}$ and DKO MEFs with TGFβ-1, a known activator

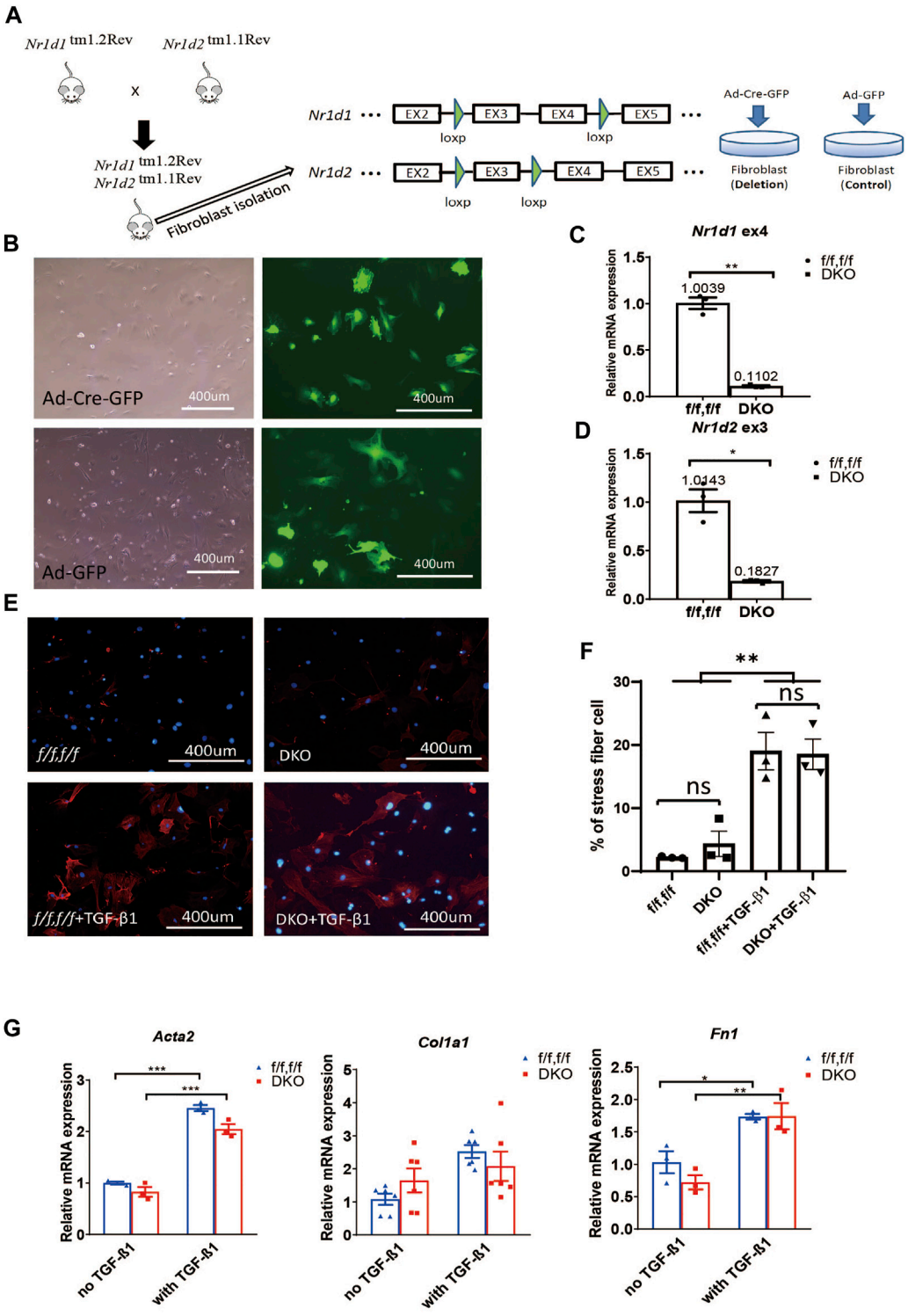

FIGURE 1
REV-ERB deletion does not affect MEFs activation. **(A)** Schematic illustration of the strategy to create fibroblasts (MEFs and CFs) models *in vitro*. *Nr1d1*$^{tm1.2Rev}$ and *Nr1d2*$^{tm1.1Rev}$ double floxed (*Nr1d1/2* $^{fl/fl}$) mouse line were generated by crossing. MEFs or CFs were isolated from double floxed mice, and REV-ERB was depleted by infection with Ad-Cre-GFP or Ad-GFP as control. Green triangle: loxP site. **(B)** Representative phase-contrast and GFP fluorescence images of MEFs from *Nr1d1/2* $^{fl/fl}$ mouse infected with Ad-Cre-GFP or Ad-GFP virus. **(C,D)** Relative mRNA expression of *Nr1d1* or *Nr1d2* with qRT-PCR primers spanning the loxP sites n = 3. **(E)** Representative images of immunostaining using α-SMA (Red) and DAPI (Blue) for *Nr1d1/2* $^{fl/fl}$ (control) and DKO MEFs with or without TGFβ-1 treatment. **(F)** Quantification of the percentage of the stress fiber positive cells in *Nr1d1/2* $^{fl/fl}$ (control) and DKO MEFs with or without TGFβ-1 treatment. Stress fiber was indicated by α-SMA staining. N = 3. **(G)** Relative mRNA expression of *Acta2*, *Col1a1,* and *Fn1* in *Nr1d1/2* $^{fl/fl}$ and DKO MEFs with or without TGFβ-1 treatment. *n*=3 to 6.*p = 0.05, ***p < 0.001, and ****p < 0.0001 by 2-sided Student's t-test **(C,D)** and *P < 0.05, **P < 0.01 and ***P < 0.001 by two-way ANOVA **(F,G)**. Data are presented as mean ± SEM.

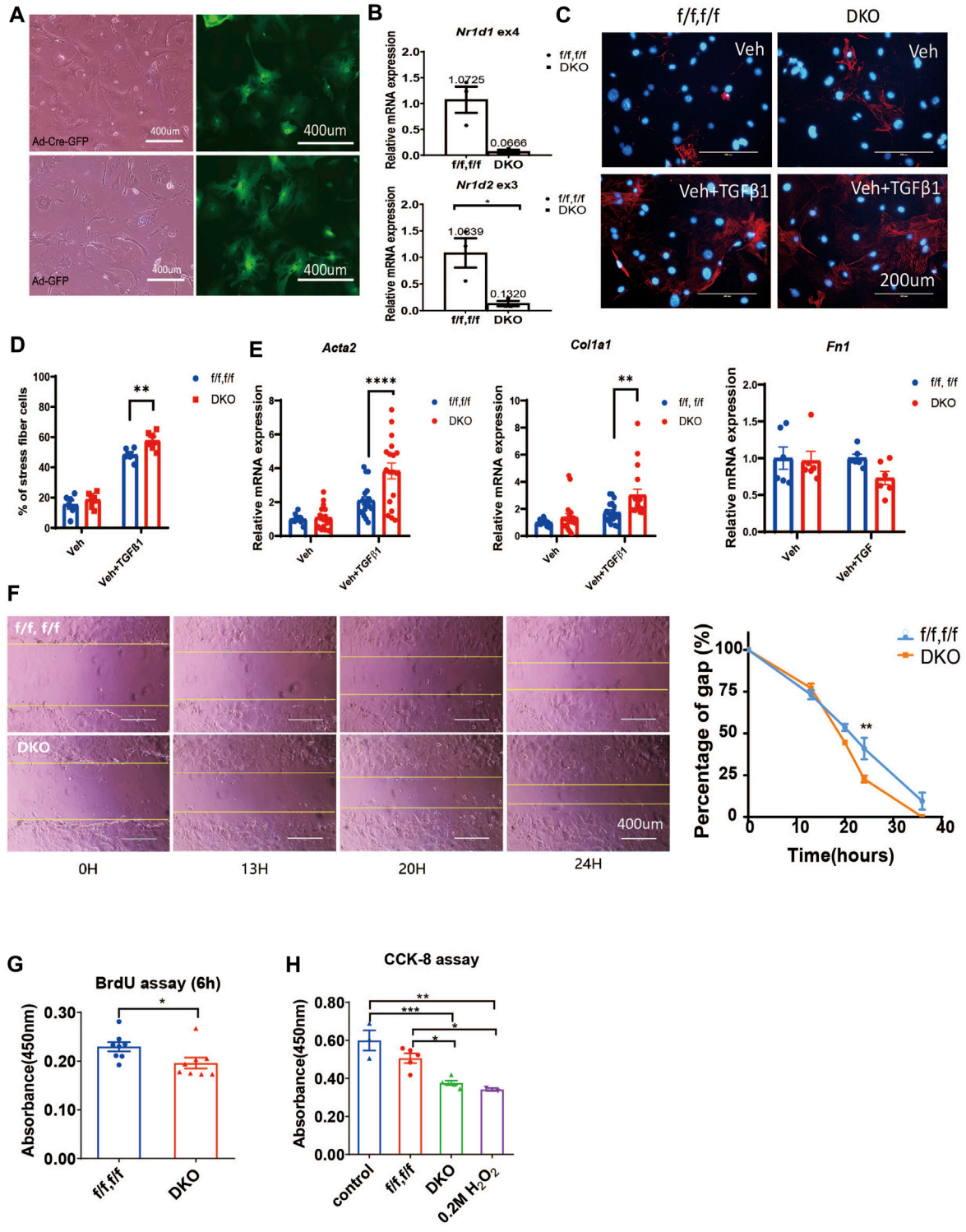

FIGURE 2
REV-ERB deletion leads to exaggerated activation of CFs. **(A)** Representative phase-contrast and GFP fluorescence images of CFs from *Nr1d1/2* $^{fl/fl}$ mouse infected with Ad-Cre-GFP or Ad-GFP virus. **(B)** Relative mRNA expression of *Nr1d1* and *Nr1d2* with qRT-PCR primers spanning loxP sites *n*=3. **(C)** Representative images of immunostaining of α-SMA (Red) and DAPI (Blue) for *Nr1d1/2* $^{fl/fl}$ (control) and DKO CFs with or without TGFβ-1 treatment. **(D)** Quantification of stress fiber positive cells in *Nr1d1/2* $^{fl/fl}$ (control) and DKO CFs with or without TGFβ-1 treatment *n*=6. **(E)** Relative mRNA expression of *Acta2*, *Col1a1,* and *Fn1* in *Nr1d1/2* $^{fl/fl}$ and DKO CFs with or without TGFβ-1 treatment *n*=6 to 18. **(F)** Representative images and quantification of the wound healing assay at different time points of the *Nr1d1/2* $^{fl/fl}$ and DKO CFs, n = 3, data are presented as mean ± SEM. **(G)** BrdU assay. The absorbance of BrdU incorporation was measured at 450 nm after 6 h incubation for *Nr1d1/2* $^{fl/fl}$ and DKO CFs, n = 8. **(H)** CCK-8 assay. The absorbance was measured at 450 nm for *Nr1d1/2* $^{fl/fl}$ and DKO CFs after 5h incubation with the WST-8 solution, n = 5. **p* = 0.05, ****p* < 0.001, and *****p* < 0.0001 by one-way ANOVA **(H)**, two-way ANOVA **(D–F)**, and 2-sided Student's t-test **(B and G)**. Data are presented as mean ± SEM.

of MEFs *in vitro* (Leask, 2010; Dobaczewski et al., 2011). By immunostaining of the activated fibroblasts/myofibroblasts marker αSMA, we found there is a minimum signal of αSMA at the baseline for both the *Nr1d1/2*$^{fl/fl}$ and DKO MEFs. 48 h after treatment with TGFβ-1, both *Nr1d1/2*$^{fl/fl}$ and DKO MEFs showed similarly increased αSMA signals (Figures 1E,F). To further quantify the levels of fibroblasts activation in the TGFβ-1 treated *Nr1d1/2*$^{fl/fl}$ and DKO MEFs, we examined several myofibroblasts markers by qRT-PCR. The relative expression level of alpha smooth actin (*Acta2*), collagen I (*Col1a1*), and fibronectin (*Fn1*) were determined in *Nr1d1/2*$^{fl/fl}$ and DKO MEFs with or without TGFβ-1 treatment. Consistent with immunofluorescent staining of αSMA, the qRT-PCR of all three myofibroblasts markers showed a significant effect of TGFβ-1 in fibroblasts activation, but there is no difference between the *Nr1d1/2*$^{fl/fl}$ and DKO MEFs either in baseline or TGFβ-1 treated conditions (Figure 1G). Our results suggested that REV-ERB activity was not involved in MEFs activation upon TGFβ-1 stimulation.

Double deletion of *Nr1d1*/*Nr1d2* enhances the CFs activation

Surprised by the results in MEFs, we went on to determine if REV-ERB plays a role in cardiac fibroblasts (CFs) activation. We isolated primary CFs from *Nr1d1/2*$^{fl/fl}$ mice and infected them with Cre expressing (Ad-Cre-GFP) or control (Ad-GFP) adenovirus. Infection efficiency was near 100%, and we found that the adenovirus induced Cre expression results in a 94% reduction of *Nr1d1* and an 87% reduction of *Nr1d2* in the ad-Cre-GFP infected CFs (Figures 2A,B). TGFβ-1 treatment was used to stimulate cardiac fibroblasts activation, immunostaining of the αSMA and qRT-PCR was performed on myofibroblasts markers. Interestingly, we found that while there is no difference at baseline, the DKO CFs showed higher αSMA signal positive cells compared to the control group with TGFβ-1 activation (Figures 2C,D). Consistent with this finding, the TGFβ-1 treatment induced higher expression of myofibroblasts markers *Acta2* and *Col1a1* but not *Fn1* in DKO CFs (Figure 2E).

We then further investigated the effect of REV-ERB on CF activation functionally, we performed wound healing, proliferation, and viability assays in the control *Nr1d1/2*$^{fl/fl}$ and DKO CFs. DKO CFs displayed a faster wound healing compared to the control *Nr1d1/2*$^{fl/fl}$ CFs with a significant difference at 24 h after the initial scratch, suggesting an increased proliferation, migration, and/or reduced death of the REV-ERB DKO CFs (Figure 2F). We then compared control *Nr1d1/2*$^{fl/fl}$ and DKO CFs in a BrdU incorporation assay to assess proliferation and in a CCK-8 assay for viability. Interestingly, DKO CFs showed both reduced proliferation and viability, which does not support faster wound-healing (Figures 2G,H). Taken together, we found DKO CFs showed reduced proliferation and viability but increased migration ability and increased fibroblast activation with TGFβ-1 treatment.

SR9009 inhibits CFs activation

SR9009 has been shown to provide numerous health benefits in a variety of preclinical disease models *in vivo* (Zhang et al., 2017; Ishimaru et al., 2019; Reitz et al., 2019; Cunningham et al., 2020; Wolff et al., 2020). In particular, SR9009 offered cardioprotection in both pressure overload and ischemia-reperfusion models (Zhang et al., 2017; Reitz et al., 2019). Fibrosis was also significantly reduced by SR9009 post pressure overload (Zhang et al., 2017). However, whether the reduced cardiac fibrosis post pressure overload is a result of reduced cardiac injury or a direct effect of SR9009 on CFs remains unknown. Similarly, anti-fibrotic effect of SR9009 was observed in pulmonary and hepatic models (Cunningham et al., 2020; Griffett et al., 2020), suggesting that SR9009 might have a direct effect on fibrosis and that its anti-fibrotic effect in the heart may be independent of the myocyte injury.

We treated the neonatal rat CFs with SR9009 in the presence or absence of TGFβ-1. We found that activation of CFs was completely blocked by SR9009 measured by immunostaining of αSMA (Figures 3A,B). Moreover, the SR9009-treated CFs showed a significantly impaired migration activity in a scratch assay (Figures 3C,D). This is consistent with the results that DKO CFs show increased activation and faster migration (Figure 2) suggesting SR9009 may work as an agonist of REV-ERB to inhibit CFs activation.

SR9009 inhibits CFs and MEFs activation independent of REV-ERB

We then went on to test if the effect of SR9009 on fibroblasts is REV-ERB dependent. We treated *Nr1d1/2*$^{fl/fl}$ and DKO CFs or MEFs with or without TGFβ-1 and SR9009. Immunostaining of the αSMA was performed in CFs, interestingly, we found that SR9009 strongly suppressed the αSMA signals at baseline for both *Nr1d1/2*$^{fl/fl}$ and DKO CFs and most impressively, SR9009 completely blocked TGFβ-1 induced myofibroblasts activation for both genotype groups (Figure 4A). Similarly, qRT-PCR of myofibroblasts markers showed that SR9009 greatly reduced all myofibroblasts markers at baseline and abolished the activation upon TGFβ-1 stimulation in CFs of both genotypes (Figure 4B). Interestingly, this SR9009 mediated suppression of myofibroblasts activation was indistinguishable between *Nr1d1/2*$^{fl/fl}$ and DKO CFs (Figure 4B), A similar effect was also observed in *Nr1d1/2*$^{fl/fl}$ and DKO MEFs (Figure 4C), demonstrating that the SR9009 effect in inhibiting fibroblasts activation is independent of REV-ERB.

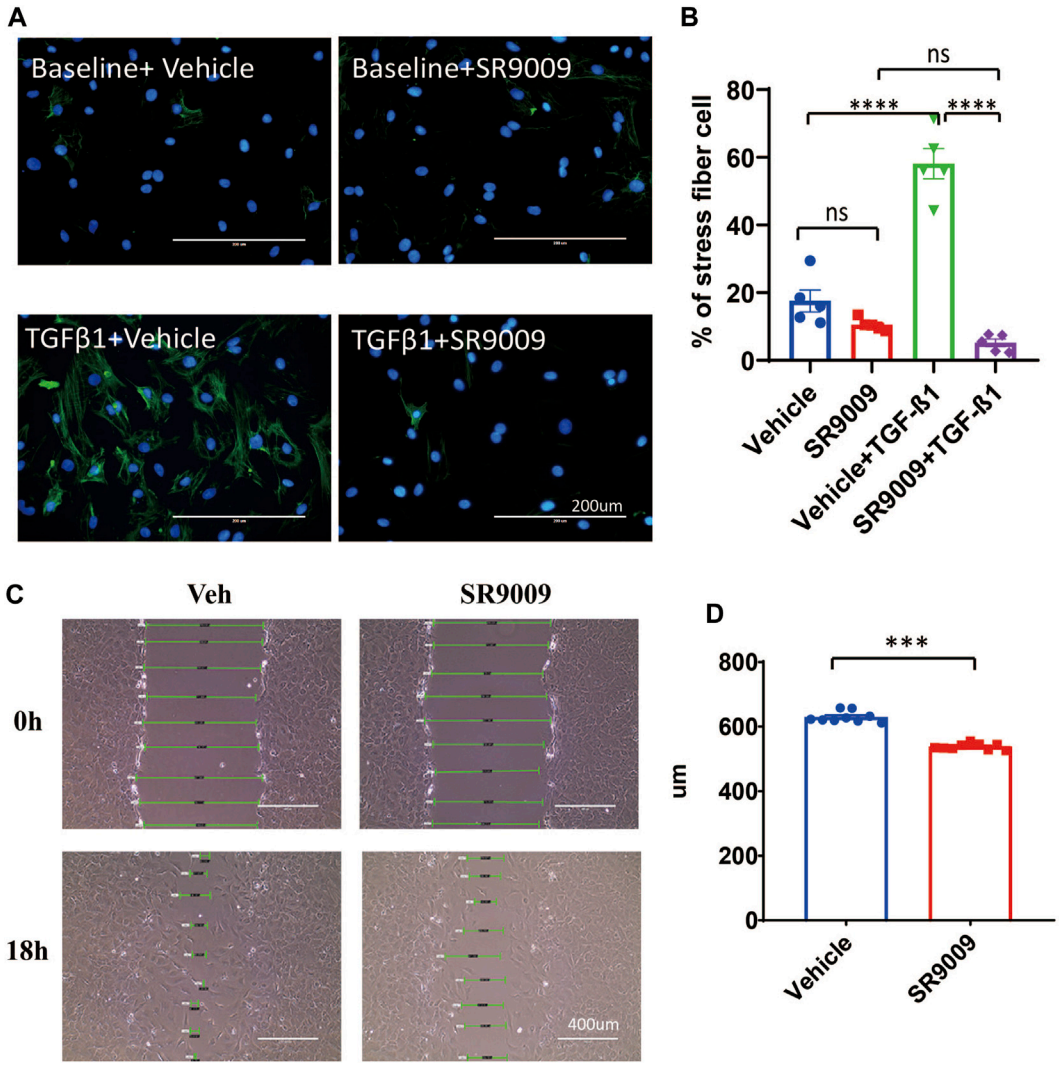

FIGURE 3
SR9009 inhibits CFs activation. **(A)** Representative immunostaining images showing α-SMA (Green) and DAPI (Blue) in vehicle or SR9009 treated CFs with or without TGFβ-1 treatment. **(B)** Quantification of the percentage of the stress fiber positive cells in vehicle or SR9009 treated CFs with or without TGFβ-1 treatment. Stress fiber was indicated by α-SMA staining, $n = 5$. **(C)** Representative images wound healing assay of CFs with or without SR9009 treatment at 0 and 18 h. **(D)** Quantification of the gap distance of the CFs treated with vehicle or SR9009 in the wound healing assay, $n = 9$. $^{*}p = 0.05$, $^{***}p < 0.001$, and $^{****}p < 0.0001$ by one-way ANOVA **(B)** and 2-sided Student's t-test **(D)**. Data are presented as mean ± SEM.

Discussion

The cardiac protecting role of a circadian core clock factor, REV-ERB has been first established using a pharmacological tool drug, SR9009 (Zhang et al., 2017; Reitz et al., 2019). Although the target specificity of SR9009 has been challenged later, the role of REV-ERB in the heart was confirmed by more recent reports using the REV-ERB cardiac-specific knockout murine models (Dierickx et al., 2022; Song et al., 2022). REV-ERB has shown antifibrosis effects in the cardiac pressure-overload model as well as several other models, suggesting it may have an important role of REV-ERB in the cardiac fibroblasts (Zhang et al., 2017; Gonzalez-Fernandez et al., 2018; Cunningham et al., 2020; Griffett et al., 2020). In this study, we specifically interrogated the cell-autonomous role of REV-ERB in MEFs and CFs. Surprisingly, while REV-ERB does not seem to play any significant role in the MEF activation, it is critical in keeping CFs in quiescence. REV-ERB is essential for CF survival and proliferation. However, it inhibits CFs activation and wound healing. CFs with REV-ERBα/β double deletion showed increased activation upon TGFβ-1

10.3389/fphar.2022.899628

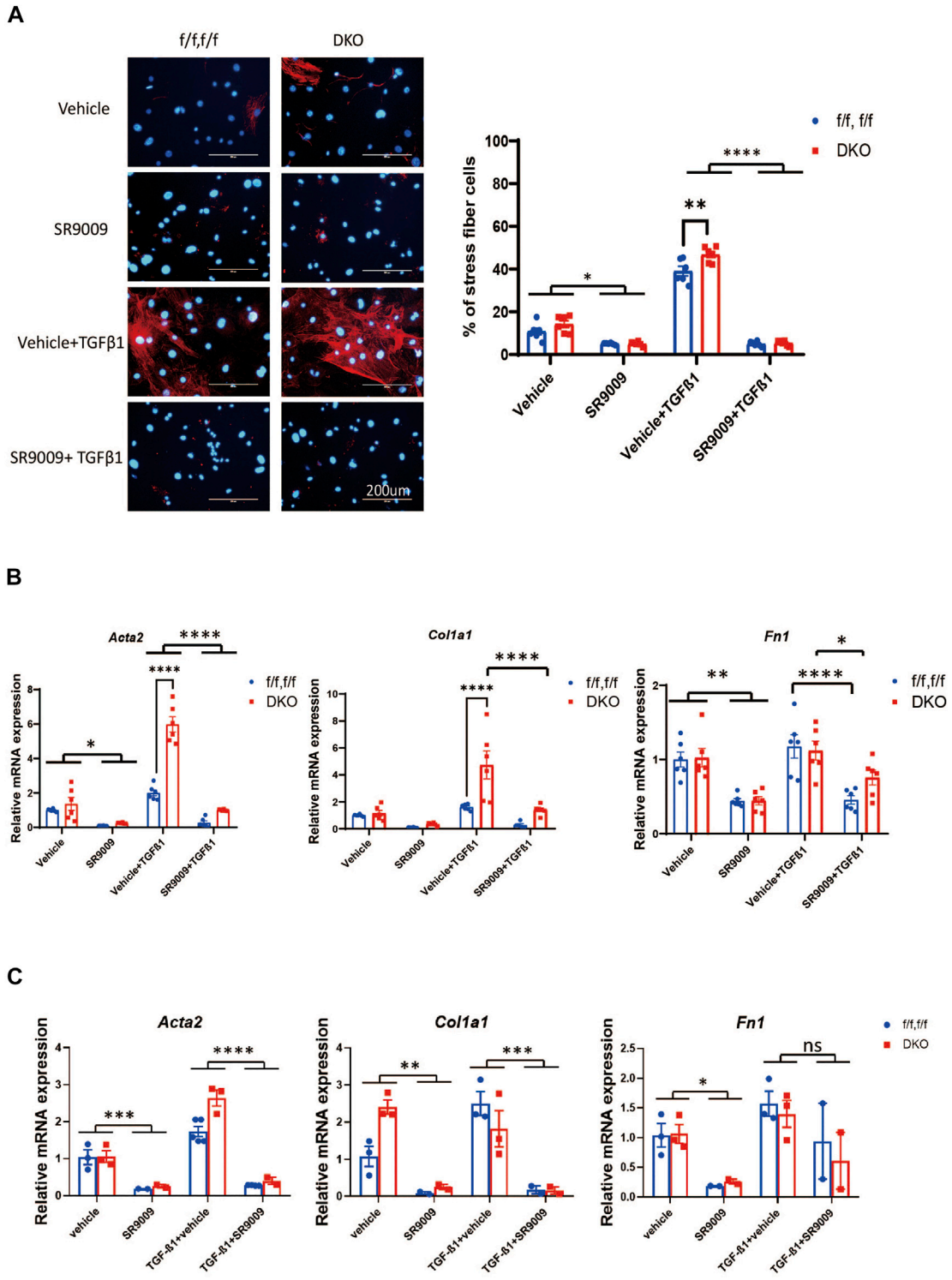

FIGURE 4
SR9009 inhibits MEFs activation independent of REV-ERB. **(A)** Representative images and quantification of immunostaining of α-SMA (Red) and DAPI (Blue) for *Nr1d1/2* $^{fl/fl}$ (control) and DKO CFs with or without SR9009 treatment and TGFβ-1 treatment n=6. **(B)** Relative mRNA expression of *Acta2*, *Col1a1*, and *Fn1* with or without SR9009 treatment in *Nr1d1/2* $^{fl/fl}$ and DKO CFs at baseline and post TGFβ-1 induced activation n=6. **(C)** Relative mRNA expression of *Acta2*, *Col1a1*, and *Fn1* with or without SR9009 treatment in *Nr1d1/2* $^{fl/fl}$ and DKO MEFs at baseline and post TGFβ-1 induced activation n=3. *p = 0.05, ***p < 0.001, and ****p < 0.0001 by two-way ANOVA, with multiple comparison corrected by Sidak, data are presented as mean ± SEM.

treatment, reduced proliferation and viability, and faster wound healing. Since both viability and proliferation are reduced, the increased would healing is likely due to increased migration. Thus, REV-ERB seems to keep CFs in a healthy quiescent state.

Its function in CFs suggests that pharmacological targeting of REV-ERB simultaneuosly in both CFs and cardiomyocytes may lead to synergistic benefits in cardiac diseases. *In vivo* testing using CF-specific REV-ERB deletion models will be the next step to further validate this hypothesis.

Our study demonstrated that REV-ERBα/β play essential roles in CFs independent of cardiomyocytes and other cell types in the heart. This function likely contributes to the cardioprotective effect of REV-ERB agonist when administered systemically. Interestingly, we also found that REV-ERB does not carry a similar function in MEFs. There are many different types of fibroblasts residing in different tissue niches. In addition to their commonality, they may assume tissue-specific function and have unique responses to different stimuli. Dissecting out their differences will be an interesting future project, which will help understand the systemic consequences of pharmacological targeting of REV-ERB.

Another interesting observation is that SR9009 has a strong suppressive effect in CFs and MEFs activation that is independent of REV-ERB. Similar results were seen in both CFs and MEFs. Our results corroborated with previous reports and showed that SR9009 likely has off-target effects that contribute to its cardiac protective and anti-fibrotic functions (Dierickx et al., 2019; Li et al., 2022). A more detailed study to identify the possible mechanisms and targets of SR9009 is beyond the scope of the current study. Novel REV-ERB agonists with enhanced specificity will be needed to facilitate future studies of REV-ERB functions. These future novel compounds should be robustly tested in REV-ERB deleted cellular or animal models.

Data availability statement

The original contributions presented in the study are included in the article/supplementary material, further inquiries can be directed to the corresponding authors.

Ethics statement

The animal study was reviewed and approved by the Institutional Animal Care and Use Committee at Baylor College of Medicine.

Author contributions

XL and LZ conceived the project. XL, SS, LQ, C-LT, HL, WX, and TH performed the experiment and analyzed the data. XL, TB, ZY, ZS, and LZ wrote the manuscript.

Funding

This work was supported by the NIH grant HL143067 (LZ). We are also thankful for HL150589, HL165270, HL153320, HL165270, DK111436, AG069966, AG070687, and ES027544, John S. Dunn Foundation, Mrs. Clifford Elder White Graham Endowed Research Fund, Cardiovascular Research Institute at BCM, the DLDCCC, the Specialized Programs of Research Excellence (SPORE) program (P50CA126752), the Gulf Coast Center for Precision Environmental Health (P30ES030285), and the Texas Medical Center Digestive Diseases Center (P30 DK056338).

Conflict of interest

The authors declare that the research was conducted in the absence of any commercial or financial relationships that could be construed as a potential conflict of interest.

Publisher's note

References

Banerjee, S., Wang, Y., Solt, L. A., Griffett, K., Kazantzis, M., Amador, A., et al. (2014). Pharmacological targeting of the mammalian clock regulates sleep architecture and emotional behaviour. *Nat. Commun.* 5, 5759. doi:10.1038/ncomms6759

Cho, H., Zhao, X., Hatori, M., Yu, R. T., Barish, G. D., Lam, M. T., et al. (2012). Regulation of circadian behaviour and metabolism by REV-ERB-α and REV-ERB-β. *Nature* 485 (7396), 123–127. doi:10.1038/nature11048

Cunningham, P. S., Meijer, P., Nazgiewicz, A., Anderson, S. G., Borthwick, L. A., Bagnall, J., et al. (2020). The circadian clock protein REVERBα inhibits pulmonary fibrosis development. *Proc. Natl. Acad. Sci. U. S. A.* 117 (2), 1139–1147. doi:10.1073/pnas.1912109117

Dierickx, P., Emmett, M. J., Jiang, C., Uehara, K., Liu, M., Adlanmerini, M., et al. (2019). SR9009 has REV-ERB-independent effects on cell proliferation and metabolism. *Proc. Natl. Acad. Sci. U. S. A.* 116 (25), 12147–12152. doi:10.1073/pnas.1904226116

Dierickx, P., Zhu, K., Carpenter, B. J., Jiang, C., Vermunt, M. W., Xiao, Y., et al. (2022). Circadian REV-ERBs repress E4bp4 to activate NAMPT-dependent NAD(+) biosynthesis and sustain cardiac function. *Nat. Cardiovasc. Res.* 1 (1), 45–58. doi:10.1038/s44161-021-00001-9

Disertori, M., Mase, M., and Ravelli, F. (2017). Myocardial fibrosis predicts ventricular tachyarrhythmias. *Trends cardiovasc. Med.* 27 (5), 363–372. doi:10.1016/j.tcm.2017.01.011

Dobaczewski, M., Chen, W., and Frangogiannis, N. G. (2011). Transforming growth factor (TGF)-beta signaling in cardiac remodeling. *J. Mol. Cell. Cardiol.* 51 (4), 600–606. doi:10.1016/j.yjmcc.2010.10.033

Durkin, M. E., Qian, X., Popescu, N. C., and Lowy, D. R. (2013). Isolation of mouse embryo fibroblasts. *Bio. Protoc.* 3 (18), e908. doi:10.21769/bioprotoc.908

Frohlich, E. D. (2001). Fibrosis and ischemia: The real risks in hypertensive heart disease. *Am. J. Hypertens.* 14 (6 2), 194S–199S. doi:10.1016/s0895-7061(01)02088-x

Gonzalez-Fernandez, B., Sanchez, D. I., Crespo, I., San-Miguel, B., de Urbina, J. O., Gonzalez-Gallego, J., et al. (2018). Melatonin attenuates dysregulation of the circadian clock pathway in mice with CCl4-induced fibrosis and human hepatic stellate cells. *Front. Pharmacol.* 9, 556. doi:10.3389/fphar.2018.00556

Griffett, K., Bedia-Diaz, G., Elgendy, B., and Burris, T. P. (2020). REV-ERB agonism improves liver pathology in a mouse model of NASH. *PLoS One* 15 (10), e0236000. doi:10.1371/journal.pone.0236000

Ingle, K. A., Kain, V., Goel, M., Prabhu, S. D., Young, M. E., and Halade, G. V. (2015). Cardiomyocyte-specific Bmal1 deletion in mice triggers diastolic dysfunction, extracellular matrix response, and impaired resolution of inflammation. *Am. J. Physiol. Heart Circ. Physiol.* 309 (11), H1827–H1836. doi:10.1152/ajpheart.00608.2015

Ishimaru, K., Nakajima, S., Yu, G., Nakamura, Y., and Nakao, A. (2019). The putatively specific synthetic REV-ERB agonist SR9009 inhibits IgE- and IL-33-mediated mast cell activation independently of the circadian clock. *Int. J. Mol. Sci.* 20 (24), E6320. doi:10.3390/ijms20246320

Jellis, C., Martin, J., Narula, J., and Marwick, T. H. (2010). Assessment of nonischemic myocardial fibrosis. *J. Am. Coll. Cardiol.* 56 (2), 89–97. doi:10.1016/j.jacc.2010.02.047

Kakkar, R., and Lee, R. T. (2010). Intramyocardial fibroblast myocyte communication. *Circ. Res.* 106 (1), 47–57. doi:10.1161/CIRCRESAHA.109.207456

Karch, J., Bround, M. J., Khalil, H., Sargent, M. A., Latchman, N., Terada, N., et al. (2019). Inhibition of mitochondrial permeability transition by deletion of the ANT family and CypD. *Sci. Adv.* 5 (8), eaaw4597. doi:10.1126/sciadv.aaw4597

Leask, A. (2010). Potential therapeutic targets for cardiac fibrosis: TGFbeta, angiotensin, endothelin, CCN2, and PDGF, partners in fibroblast activation. *Circ. Res.* 106 (11), 1675–1680. doi:10.1161/CIRCRESAHA.110.217737

Lefta, M., Campbell, K. S., Feng, H. Z., Jin, J. P., and Esser, K. A. (2012). Development of dilated cardiomyopathy in Bmal1-deficient mice. *Am. J. Physiol. Heart Circ. Physiol.* 303 (4), H475–H485. doi:10.1152/ajpheart.00238.2012

Li, H., Song, S., Tien, C. L., Qi, L., Graves, A., Nasiotis, E., et al. (2022). SR9009 improves heart function after pressure overload independent of cardiac REV-ERB. *Front. Cardiovasc. Med.* 9, 952114. doi:10.3389/fcvm.2022.952114

Liang, C. C., Park, A. Y., and Guan, J. L. (2007). *In vitro* scratch assay: A convenient and inexpensive method for analysis of cell migration *in vitro*. *Nat. Protoc.* 2 (2), 329–333. doi:10.1038/nprot.2007.30

Manabe, I., Shindo, T., and Nagai, R. (2002). Gene expression in fibroblasts and fibrosis: Involvement in cardiac hypertrophy. *Circ. Res.* 91 (12), 1103–1113. doi:10.1161/01.res.0000046452.67724.b8

Pinto, A. R., Ilinykh, A., Ivey, M. J., Kuwabara, J. T., D'Antoni, M. L., Debuque, R., et al. (2016). Revisiting cardiac cellular composition. *Circ. Res.* 118 (3), 400–409. doi:10.1161/CIRCRESAHA.115.307778

Reitz, C. J., Alibhai, F. J., Khatua, T. N., Rasouli, M., Bridle, B. W., Burris, T. P., et al. (2019). SR9009 administered for one day after myocardial ischemia-reperfusion prevents heart failure in mice by targeting the cardiac inflammasome. *Commun. Biol.* 2, 353. doi:10.1038/s42003-019-0595-z

Song, S., Tien, C. L., Cui, H., Basil, P., Zhu, N., Gong, Y., et al. (2022). Myocardial rev-erb-mediated diurnal metabolic rhythm and obesity paradox. *Circulation* 145 (6), 448–464. doi:10.1161/CIRCULATIONAHA.121.056076

Stujanna, E. N., Murakoshi, N., Tajiri, K., Xu, D., Kimura, T., Qin, R., et al. (2017). Rev-erb agonist improves adverse cardiac remodeling and survival in myocardial infarction through an anti-inflammatory mechanism. *PLoS One* 12 (12), e0189330. doi:10.1371/journal.pone.0189330

Takahashi, J. S. (2017). Transcriptional architecture of the mammalian circadian clock. *Nat. Rev. Genet.* 18 (3), 164–179. doi:10.1038/nrg.2016.150

Travers, J. G., Kamal, F. A., Robbins, J., Yutzey, K. E., and Blaxall, B. C. (2016). Cardiac fibrosis: The fibroblast awakens. *Circ. Res.* 118 (6), 1021–1040. doi:10.1161/CIRCRESAHA.115.306565

Wang, Q., Sundar, I. K., Lucas, J. H., Muthumalage, T., and Rahman, I. (2021). Molecular clock REV-ERBα regulates cigarette smoke-induced pulmonary inflammation and epithelial-mesenchymal transition. *JCI Insight* 6 (12), 145200. doi:10.1172/jci.insight.145200

Wolff, S. E. C., Wang, X. L., Jiao, H., Sun, J., Kalsbeek, A., Yi, C. X., et al. (2020). The effect of rev-erbα agonist SR9011 on the immune response and cell metabolism of microglia. *Front. Immunol.* 11, 550145. doi:10.3389/fimmu.2020.550145

Young, M. E., Brewer, R. A., Peliciari-Garcia, R. A., Collins, H. E., He, L., Birky, T. L., et al. (2014). Cardiomyocyte-specific BMAL1 plays critical roles in metabolism, signaling, and maintenance of contractile function of the heart. *J. Biol. Rhythms* 29 (4), 257–276. doi:10.1177/0748730414543141

Zhang, L., Zhang, R., Tien, C. L., Chan, R. E., Sugi, K., Fu, C., et al. (2017). REV-ERBα ameliorates heart failure through transcription repression. *JCI Insight* 2 (17), 95177. doi:10.1172/jci.insight.95177

Zhou, P., and Pu, W. T. (2016). Recounting cardiac cellular composition. *Circ. Res.* 118 (3), 368–370. doi:10.1161/CIRCRESAHA.116.308139